STAR Protocols

CellPress
OPEN ACCESS

Protocol

Synthesis of Zr metal–organic frameworks (MOFs) to remove Fe^{3+} from water

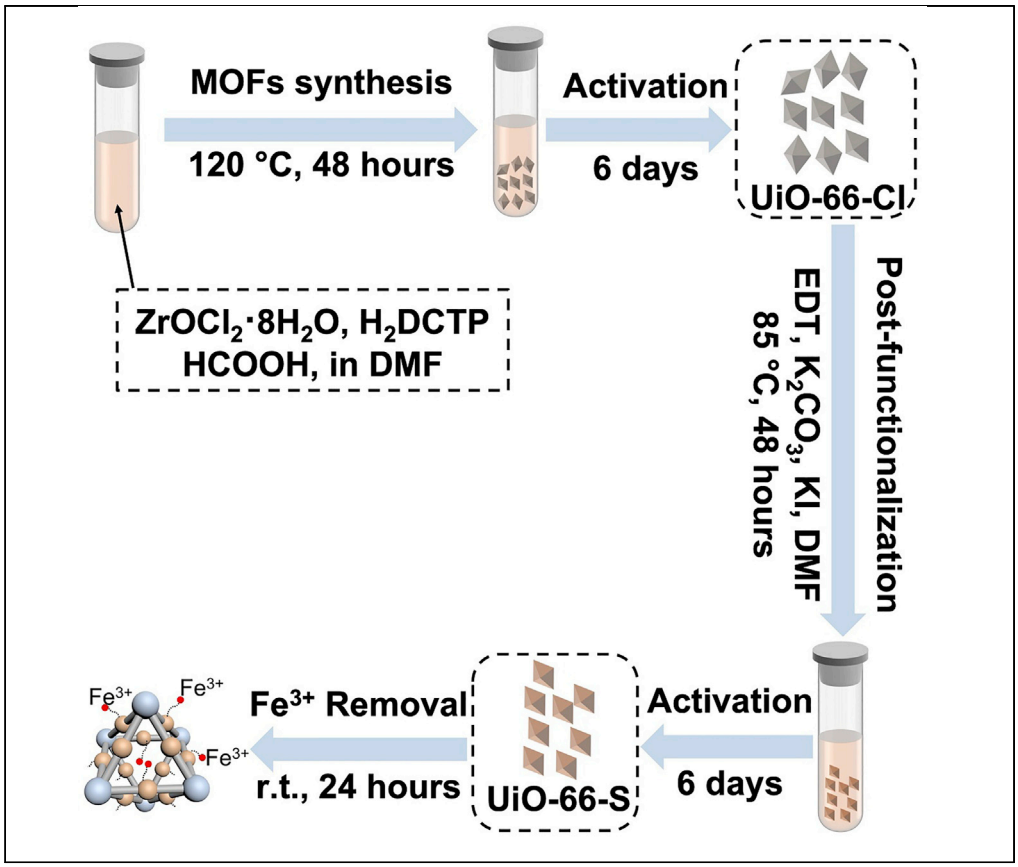

Although a trace amount of Fe^{3+} is essential for human physiological function, excessive amounts are lethal. Here, we present a protocol for removing Fe^{3+} from water through highly crystalline and stable thiol-functionalized Zr metal-organic frameworks (Zr-MOFs). We provide details of the MOFs synthesis and post-functionalization procedures, and include key performance data of the Zr-MOFs for removing Fe^{3+}, which were collected from the inductively coupled plasma-optical emission spectrometer (ICP-OES) and inductively coupled plasma mass spectrometer (ICP-MS).

Publisher's note: Undertaking any experimental protocol requires adherence to local institutional guidelines for laboratory safety and ethics.

Yufei Yuan,
Yoonseob Kim

yoonseobkim@ust.hk

Highlights

UiO-66-Cl synthesis from $ZrOCl_2 \cdot 8H_2O$ and 2,5-dichloroterephthalic acid

UiO-66-Cl post-functionalized with 1,2-ethanedithiol to obtain UiO-66-S

Detailed characterization of Zr-MOFs

UiO-66-S removes Fe^{3+} from water

Yuan & Kim, STAR Protocols 3, 101477
September 16, 2022 https://doi.org/10.1016/j.xpro.2022.101477

STAR Protocols

CellPress
OPEN ACCESS

Protocol

Synthesis of Zr metal–organic frameworks (MOFs) to remove Fe^{3+} from water

Yufei Yuan[1] and Yoonseob Kim[1,2,3,*]

[1]Department of Chemical and Biomolecular Engineering, The Hong Kong University of Science and Technology, Clear Water Bay, Kowloon, Hong Kong SAR, China

[2]Technical contact

[3]Lead contact

*Correspondence: yoonseobkim@ust.hk
https://doi.org/10.1016/j.xpro.2022.101477

SUMMARY

Although a trace amount of Fe^{3+} is essential for human physiological function, excessive amounts are lethal. Here, we present a protocol for removing Fe^{3+} from water through highly crystalline and stable thiol-functionalized Zr metal-organic frameworks (Zr-MOFs). We provide details of the MOFs synthesis and post-functionalization procedures, and include key performance data of the Zr-MOFs for removing Fe^{3+}, which were collected from the inductively coupled plasma-optical emission spectrometer (ICP-OES) and inductively coupled plasma mass spectrometer (ICP-MS).

For complete details on the use and execution of this protocol, please refer to Yuan et al. (2022).

BEFORE YOU BEGIN

Iron is one of the essential nutrients which maintains various human physiological functions. However, an excess amount of Fe^{3+} can induce various biological disorders. Specifically, 20–60 mg L^{-1} Fe^{3+} can damage DNA and cellular components, leading to hemochromatosis, liver cirrhosis, diabetes, and heart disease (Hartmann et al., 2013; Khatri et al., 2017). A concentration of Fe^{3+} > 200 mg L^{-1} induces severe Fe^{3+} poisoning, leading to death. Therefore, it is crucial to exploit technology that can purify the Fe^{3+} contaminated water to a drinkable level (< 0.3 mg L^{-1}) (WHO World Health Organization, 2003). Compared with water purification methods such as ion exchange, precipitation, electrodialysis, coagulation, and flocculation, adsorption is the most promising feature high removal efficiency, improved recyclability, and cost-effectiveness (Duan et al., 2018; Gabarrón et al., 2016; Nemati et al., 2017; Sun et al., 2018). Therefore, plenty of research interests focus on the synthesis of novel adsorbent. MOFs have the merits of high specific surface area and facile tunable structure, ensuring high removal efficiency for toxic heavy metal ions. Hence, MOFs are prominent for water purification compared with traditional activated carbon and zeolites (Hui et al., 2005; Wang et al., 2009). However, the aqueous stability restricts the application of the MOFs. One solution to improve the stability is synthesizing MOFs from a hard Lewis acid, a hard Lewis base pair, or a soft Lewis acid, and a soft Lewis base pair (Feng et al., 2018; Huang et al., 2020; Yuan et al., 2018a, 2018b). The Zr-based UiO-66 type MOFs have demonstrated high stability in various environments but low water purification efficiency. Therefore, in this protocol, we synthesize UiO-66 type MOFs from the Zr cluster and 2,5-dichloroterephthalic acid ($H_2BDC\text{-}Cl_2$) under solvothermal conditions and then further post-functionalize with 1,2-Ethanedithiol (EDT) (Scheme 1) to introduce the thiol chelation groups to boost the Fe^{3+} removal efficiency. Further knowledge of solvothermal synthesis and post-functionalization procedures can be found in the literature (Yuan et al., 2022).

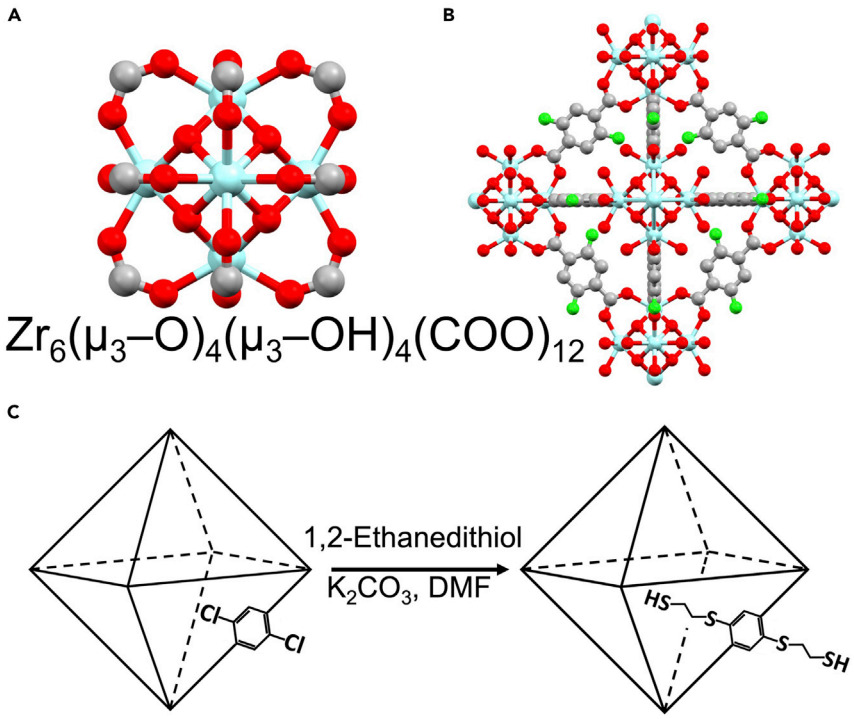

Scheme 1. Synthesis of UiO-66 MOF and post functionalization

Oxygen is shown in red; zirconium in light blue; carbon in gray; and chlorine in green. Hydrogen is omitted. Reproduced with permission (Yuan et al., 2022); Copyright, 2022 Elsevier Inc.

Preparation of stock solution

Timing: 30 min

1. Slowly add 113.44 mL 65% HNO_3 to 2000 mL of deionized water under vigorous stirring to obtain 5% HNO_3.

⚠ CRITICAL: Nitric acid is a corrosive chemical; thus, it should be handled in the fume hood. Also, the nitric acid solution should be stored in a glass container, tightly closed and well-ventilated place at room temperature.

2. Weight 101 mg lead (II) nitrate, 163.1 mg iron (III) nitrate nonahydrate, 133.1 mg cadmium nitrate tetrahydrate, 174.5 mg magnesium nitrate hexahydrate, 126.5 mg copper (II) nitrate hemi(pentahydrate), and 160.2 mg zinc nitrate hexahydrate to 100 mL 5% HNO_3 separately to obtain 1000 ppm Pb^{2+}, Fe^{3+}, Cd^{2+}, Mg^{2+}, Cu^{2+}, Zn^{2+} stock solution.
3. Add 1 mL 1000 ppm Pb^{2+}, Fe^{3+}, Cd^{2+}, Mg^{2+}, Cu^{2+}, Zn^{2+} As (V) (AsO_4^{3-}), Cd^{2+}, and Cr (VI) ($Cr_2O_7^{2-}$) stock solution to 99 mL 5% HNO_3 separately to obtain 10 ppm Pb^{2+}, Fe^{3+}, Cd^{2+}, Mg^{2+}, Cu^{2+}, Zn^{2+} As (V) (AsO_4^{3-}), Cd^{2+}, and Cr (VI) ($Cr_2O_7^{2-}$) stock solution. The stock solution should be stored in a glass container, tightly closed, and well ventilated at room temperature.

KEY RESOURCES TABLE

REAGENT or RESOURCE	SOURCE	IDENTIFIER
Chemicals, peptides, and recombinant proteins		
Zirconyl chloride octahydrate (98%)	Sigma-Aldrich	CAS: 13520-92-8
2,5-dichloroterephthalic acid (H_2DCTP, 98%)	Energy Chemical	CAS: 13799-90-1

(*Continued on next page*)

Continued

REAGENT or RESOURCE	SOURCE	IDENTIFIER
N,N-dimethylformamide (DMF, 99.8%, min)	RCI Labscan	CAS: 68-12-2
Formic acid (98%–100%)	Scharlau	CAS: 64-18-6
1,2-Ethanedithiol (EDT, ≥98%)	Sigma-Aldrich	CAS: 540-63-6
Potassium carbonate (≥99.0%)	Sigma-Aldrich	CAS: 584-08-7
Lead (II) nitrate (≥99.0%)	Sigma-Aldrich	CAS: 10099-74-8
Iron (III) nitrate nonahydrate (≥98%)	Sigma-Aldrich	CAS: 7782-61-8
Cadmium nitrate tetrahydrate (98%)	Sigma-Aldrich	CAS: 10022-68-1
Magnesium nitrate hexahydrate (99%)	Sigma-Aldrich	CAS: 13446-18-9
Copper (II) nitrate hemi(pentahydrate) (98%)	Sigma-Aldrich	CAS: 19004-19-4
Zinc nitrate hexahydrate (98%)	Sigma-Aldrich	CAS: 10196-18-6
Potassium iodide (≥99.0%)	Sigma-Aldrich	CAS: 7681-11-0
1000 ppm chromium stock solution	High-Purity Standards Inc.	SKU: 100012-1
1000 ppm arsenic stock solution	High-Purity Standards Inc.	SKU: 10003-1
Acetone (min. 99.5%)	RCI Labscan	CAS: 67-64-1
Nitric Acid (≥65%)	Honeywell/Fluka	CAS: 7697-37-2
Other		
Screw-capped glass jar	Synthware Co., Ltd	N/A
Sonicator	Branson Co., Ltd	N/A
Oven	Shanghai Yiheng Co., Ltd (Shanghai, China)	N/A
Stir plate	Heidolph Co., Ltd	P/N: 505-30000-00
Centrifuge	Centurion Scientific Co., Ltd	K3
Hot plate	Heidolph Co., Ltd	P/N: 505-30000-00
Schlenk line	Synthware Co., Ltd	N/A
Inductively coupled plasma mass spectrometer (ICP-MS)	Agilent Co., Ltd	7800
Thermo gravimetric analyzer	PerkinElmer Co., Ltd	UNIX/TGA7
Inductively coupled plasma–optical emission spectrometer (ICP-OES)	PerkinElmer Co., Ltd	7300DV
Fourier-transform infrared spectrometer (FTIR)	Thermo Fisher Scientific Co., Ltd	Nicolet IS50
JSM-7100F field emission scanning electron microscope	JEOL (Europe) BV Co., Ltd	JSM-7100F
Analytical x-ray diffractometer	Malvern Panalytical Co., Ltd	X'pert Pro
JSX-3201Z (JEOL) X-ray fluorescence spectrometer	JEOL Co., Ltd	JSX-3201Z
400 MHz Bruker NMR spectrometer	Bruker	N/A
Gas chromatography-mass spectrometer	Thermo Fisher Scientific Co., Ltd	N/A
Surface area and pore size distribution analyzer	Microtrac Co., Ltd	BELSORP MINI X

⚠ CRITICAL: 1,2-Ethanedithiol has a strong and unpleasant odor; handle it inside the fume hood.

Alternatives: We use the screw-capped glass jar for MOFs synthesis in this protocol. However, alternative tools such as autoclaves can also be used.

Optional: The resources listed above were only based on our experience. The chemicals and resources obtained from reliable commercial sources are feasible.

STEP-BY-STEP METHOD DETAILS

MOFs synthesis

Timing: 48 h

The initial step for the synthesis of UiO-66-S is the UiO-66-Cl synthesis. We synthesize UiO-66-Cl via a solvothermal method; the details are listed below (Figure 1).

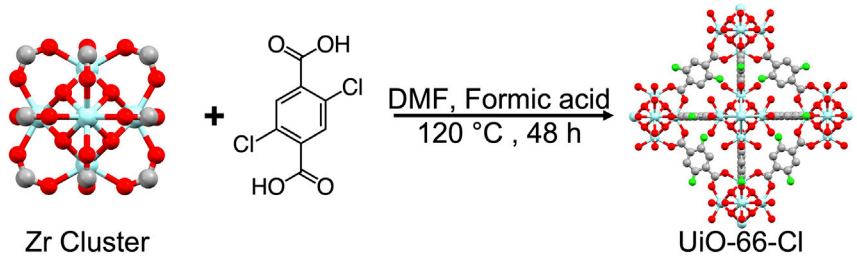

Figure 1. Synthetic procedure for the UiO-66-Cl

Oxygen is shown in red; zirconium in light blue; carbon in gray; and chlorine in green. Hydrogen is omitted. Solvothermal conditions can yield highly crystalline MOFs in 48 h. Reproduced with permission (Yuan et al., 2022); Copyright, 2022 Elsevier Inc.

1. Weigh 13.2 mg (0.041 mmol) Zirconyl chloride octahydrate and 9.6 mg (0.041 mmol) 2,5-dichloroterephthalic acid to a screw-capped glass jar.
2. Add 4.1 mL DMF and 0.82 mL formic acid to the jar.
3. Sonicate the mixture for 30 min until the solid is fully dissolved.
4. Put the jar in the oven and heat at 120°C for 48 h.
5. After cooling down to room temperature, collect the white-colored octahedral crystal, UiO-66-Cl, by centrifugation (Yield: 84%, based on Zr).

Activation of MOFs

Timing: 6 days

After the MOFs synthesis, remove the unreacted starting materials. In addition, replace the high boiling point solvent, DMF, inside the pore of MOFs with a low boiling point solvent that can be easily removed.

6. Immerse the as-synthesized UiO-66-Cl in 10 mL DMF and stir for three days, during which replace the DMF three times per day by centrifugation.
7. Immerse the as-synthesized UiO-66-Cl in 10 mL of anhydrous acetone and stir for three days, during which replace the anhydrous acetone three times per day by centrifugation.
8. Then dry the sample under vacuum at 100°C overnight to obtain the activated UiO-66-Cl.

Post-functionalization of UiO-66-Cl to UiO-66-S

Timing: 48 h

Use deprotonation reaction to post-functionalize the UiO-66-Cl to UiO-66-S, in which nucleophilic 1,2-Ethanedithiol easily replaces the chlorides.

9. Add 1.175 g UiO-66-Cl, 1.68 mL 1,2-Ethanedithiol, 2.764 g K_2CO_3, and 58.1 mg potassium iodide (KI) to a 50 mL reaction vial.
10. Change to the atmosphere in the reaction vial to nitrogen by Schlenk line.
11. Add 20 mL DMF to the reaction vial under a nitrogen atmosphere.
12. Heat the mixture to 85°C and keep at different times (24 h, 48 h, 72 h, 96 h, and 120 h).
13. After cooling down to room temperature, collect the product by centrifugation.
14. Wash the product with 20 mL H_2O six times.
15. Immerse the as-synthesized UiO-66-S in 10 mL DMF and stir for three days, during which replace the DMF three times per day by centrifugation.
16. Immerse the as-synthesized UiO-66-S in 10 mL of anhydrous acetone and stir for three days, during which replace the anhydrous acetone three times per day by centrifugation.

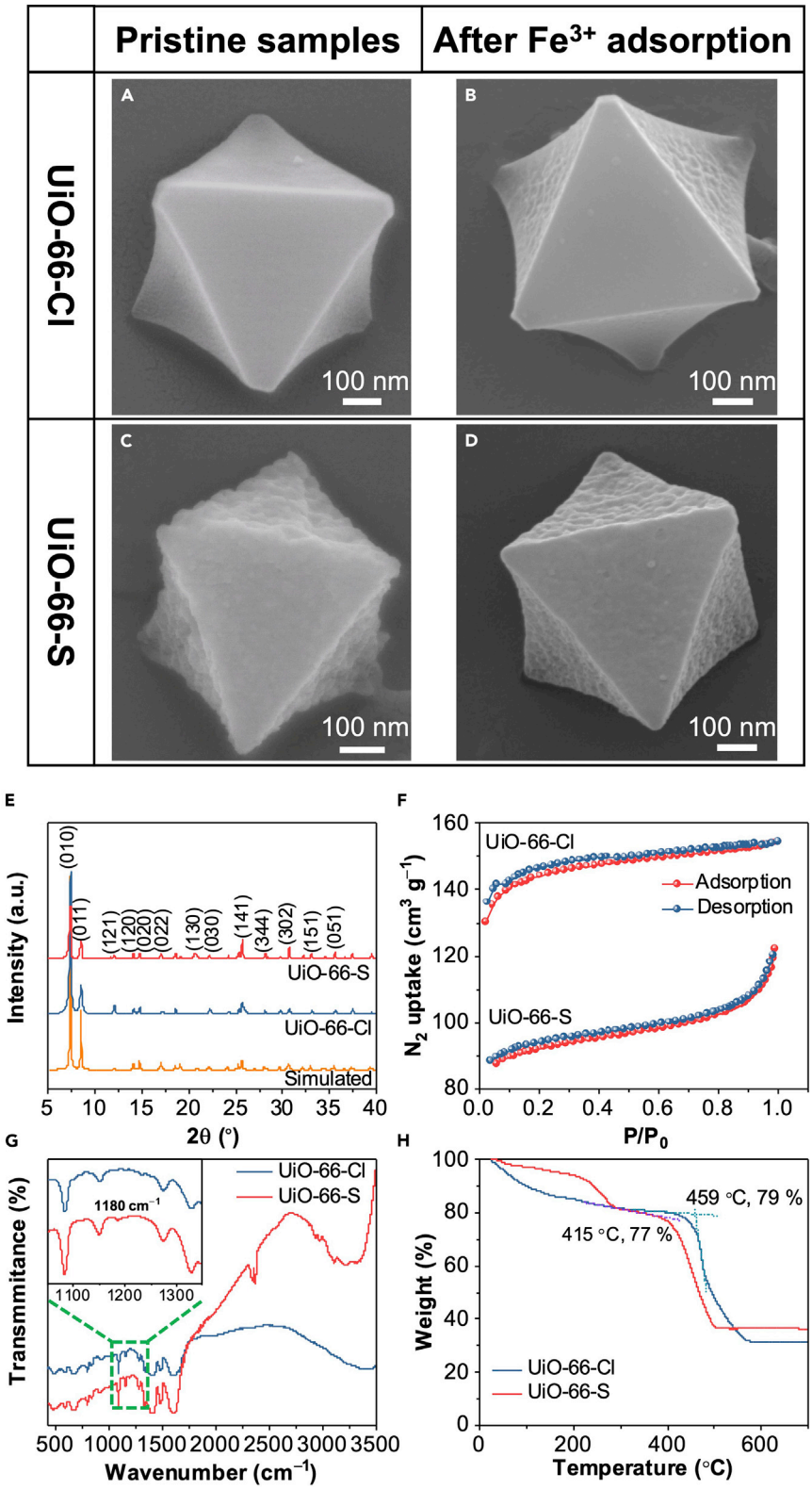
Pristine samples
After Fe3+ adsorption
UiO-66-Cl
UiO-66-S
A
B
C
D
100 nm
E
Intensity (a.u.)
(010)
(011)
(121)
(120)
(020)
(022)
(130)
(030)
(141)
(344)
(302)
(151)
(051)
UiO-66-S
UiO-66-Cl
Simulated
2θ (°)
F
UiO-66-Cl
Adsorption
Desorption
UiO-66-S
N2 uptake (cm3 g−1)
P/P0
G
1180 cm−1
UiO-66-Cl
UiO-66-S
Transmmitance (%)
Wavenumber (cm−1)
H
459 °C, 79 %
415 °C, 77 %
UiO-66-Cl
UiO-66-S
Weight (%)
Temperature (°C)

Figure 2. Characterization of UiO-66 MOFs
SEM of UiO-66-Cl and UiO-66-S before and after adsorption.
(A and B) Pristine crystal of UiO-66-Cl and crystal of UiO-66-Cl after complete Fe^{3+} adsorption.
(C and D) Pristine crystal of UiO-66-S and crystal of UiO-66-S after complete Fe^{3+} adsorption.
(E) Powder X-ray diffraction patterns of UiO-66-Cl and UiO-66-S.
(F) Nitrogen adsorption and isothermal desorption curves of the MOFs.
(G) FTIR spectra of the MOFs.
(H) TGA of the MOFs. Reproduced with permission (Yuan et al., 2022); Copyright, 2022 Elsevier Inc.

17. Then dry the sample under vacuum at 100°C overnight to obtain the activated UiO-66-S.

Characterizations of MOFs

Timing: 24 h

After the synthesis of UiO-66-Cl and UiO-66-S, use scanning electron microscopy (SEM), powder X-ray diffraction (PXRD), surface area, thermogravimetric analysis (TGA), and Fourier-transform infrared spectroscopy (FTIR) characterizations to characterize the synthesized MOFs (Figure 2). (Area et al., 1996; Mohammadinezhad and Akhlaghinia, 2019; Yuan et al., 2022).

Stability of MOFs

Timing: 35 days

Immerse the UiO-66-S and UiO-66-Cl in water (pH = 6.8), 0.1 mol L^{-1} HCl, and 0.01 mol L^{-1} NaOH aqueous solutions at room temperature for different times to investigate the stability of the MOFs (Figure 3), which demonstrate their high chemical stability (Yuan et al., 2022).

Optimization of post-functionalization

Timing: 120 h

Optimize the sulfur content in the UiO-66-S by changing the reaction time of the post-functionalization. The crystallinity is maintained during the post-functionalization process (Figure 4) (Yuan et al., 2022).

Post-functionalization – digested NMR

Timing: 2 h

Analyze the sulfur content in the UiO-66-S by the Nuclear Magnetic Resonance (NMR) spectrum of digested UiO-66-S (Figure 5). Comparing with the ^{1}H NMR spectrum of digested UiO-66-Cl, UiO-66-S shows three new peaks at δ 0.98–1.02 ppm, 3.4–3.44 ppm, and 7.09 ppm. After post-functionalization, dithiol replaces part of the Cl, resulting in the upshift of aromatic proton resonance, making a new resonance peak at 7.09 ppm. The peaks at 0.98–1.02 ppm correspond to the proton of methyl in CH_3CH_2SH, and the peaks at 3.40–3.44 ppm are the proton of -CH_2CH_2- and methylene of CH_3CH_2SH. The conversion efficiency of post-functionalization is about 43.67%. The gas chromatography-mass spectrometry results show that CH_3CH_2SH exists in the digested UiO-66-S, which results from the cleavaged C-S bond (Yuan et al., 2022).

18. Add 30.64 mg NH_4F to the mixture of 0.4 mL DMSO-d_6 and 0.2 mL D_2O to obtain the deuterated stock solution.
19. Add 10 mg UiO-66-S to the deuterated stock solution and sonicate until fully dissolved.
20. Measure the NMR spectrum by the Bruker 400 MHz NMR.

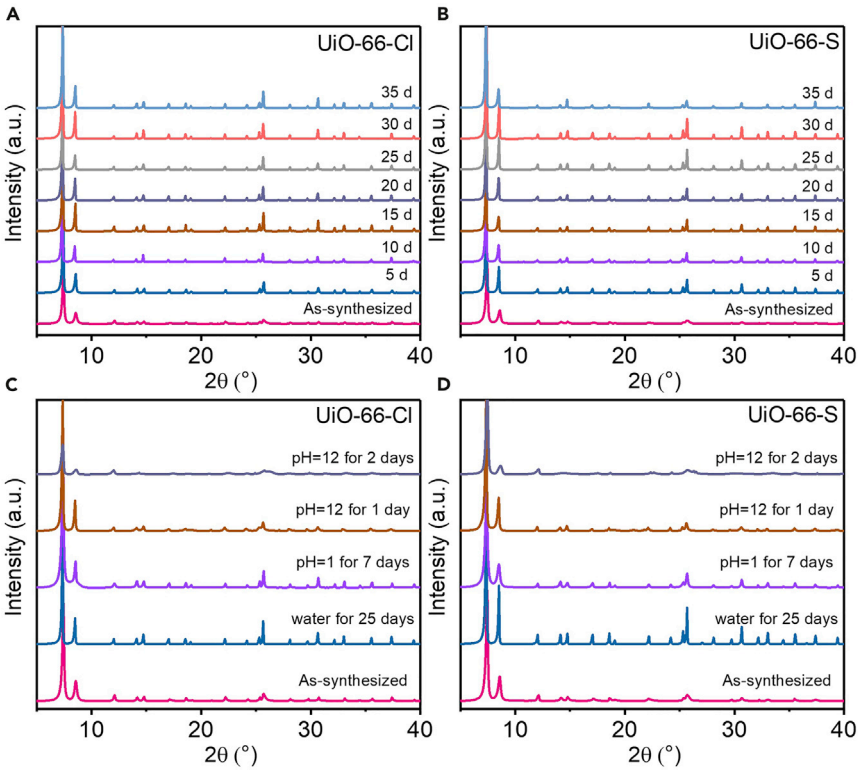

Figure 3. Stability of UiO-66 MOFs

(A and B) PXRD patterns of UiO-66-Cl and UiO-66-S after being immersed in water (A and B).

(C and D) Chemical stability of UiO-66-Cl and UiO-66-S (C and D), testing in 0.1 mol L^{-1} HCl and 0.01 mol L^{-1} NaOH. Reproduced with permission (Yuan et al., 2022); Copyright, 2022 Elsevier Inc.

21. After the NMR measurement, remove the solvent of the mixture, add the chloroform to the residual, and then filtration. The gas chromatography-mass spectrometry was conducted for the filtrate.

Ion adsorption – Uptake tests

Timing: 24 h

Use the stock solution with different concentrations (100 ppm, 200 ppm, 400 ppm, 500 ppm, 600 ppm, 800 ppm, 1000 ppm) to determine the adsorption capacity of the synthesized MOFs; details are listed below.

22. Add 10 mL Fe^{3+} stock solution with different concentrations (100 ppm, 200 ppm, 400 ppm, 500 ppm, 600 ppm, 800 ppm, 1000 ppm) to 7 batches of 20 mL glass vial.
23. Add 10 mg of as-synthesized MOFs (UiO-66-Cl or UiO-66-S) to every stock solution vial.
24. Stir the mixture for 24 h.
25. Filter the solution through a syringe filter and use the inductively coupled plasma-optical emission spectroscopy (ICP-OES) to measure the Fe^{3+} concentration in the filtrate.
26. Before running the ICP-OES test, prepare three standard stock solutions, 5% HNO_3, 500 ppm, and 1000 ppm Fe^{3+} stock solution, for calibration.
27. If the correlation coefficients (R^2) values of the calibration curve are larger than 0.9999, measure the Fe^{3+} concentration of the filtrate by ICP-OES (Figure 6A).

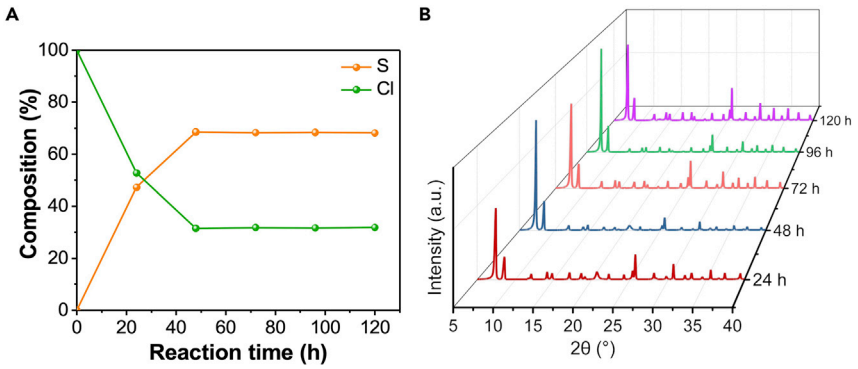

Figure 4. Optimization of UiO-66-S MOFs

(A) The sulfur content of UiO-66-S under different post-functionalization times was measured by X-ray fluorescence (XRF).

(B) PXRD pattern of the UiO-66-S with different post-functionalization times. Reproduced with permission (Yuan et al., 2022); Copyright, 2022 Elsevier Inc.

Ion adsorption – Kinetic tests

Timing: 24 h

In this protocol, we show the synthesized MOFs for heavy metal ion removal and investigate their adsorption performance, including uptake, kinetics, selectivity, and recyclability. We use the same amount of MOFs to remove the metal ions at different times to investigate the adsorption kinetics. Details are listed below.

28. Add 10 ppm Fe^{3+} stock solution to 10 batches of 20 mL glass vial, 10 mL for each vial.
29. Add 10 mg of as-synthesized MOFs (UiO-66-Cl or UiO-66-S) to every stock solution vial.
30. Stir the mixture for 20 min, 40 min, 60 min, 90 min, 2 h, 2.5 h, 3 h, 4 h, 6 h, and 8 h, respectively.
31. Filter the solution through a syringe filter and use the ICP-MS to measure the Fe^{3+} concentration in the filtrate (see Figure 7 for Fe^{3+} adsorption kinetics measurements of UiO-66-S, Methods Video S1 for UiO-66-S removing 500 ppm Fe^{3+} stock solution from 0 to 240 min, related to step 30).
32. Before running the ICP-MS test, prepare the standard stock solution, 5% HNO_3, 2.5 ppm, 5 ppm, 7.5 ppm, and 10 ppm Fe^{3+} stock solution, for calibration.
33. If the R^2 values of the calibration curve are larger than 0.9999, measure the Fe^{3+} concentration of the filtrate by ICP-MS (Figure 6B).

Ion adsorption – Selectivity tests

Timing: 24 h

We use the stock solution containing multiple metal ions to test the MOF's selectivity toward the ions.

34. Add 10 mg of as-synthesized MOFs (UiO-66-Cl or UiO-66-S) to a 20 mL glass vial.
35. Add 10 mL aqueous mixed solution (1.25 mL each 1000 ppm Fe^{3+}, As (V) (AsO_4^{3-}), Cd^{2+}, Cr (VI) ($Cr_2O_7^{2-}$), Pb^{2+}, Mg^{2+}, Cu^{2+}, Zn^{2+} stock solution) to the vial.
36. Stir the mixture for 24 h.
37. Filter the solution through a syringe filter and use the ICP-OES to measure the ion concentration in the filtrate.

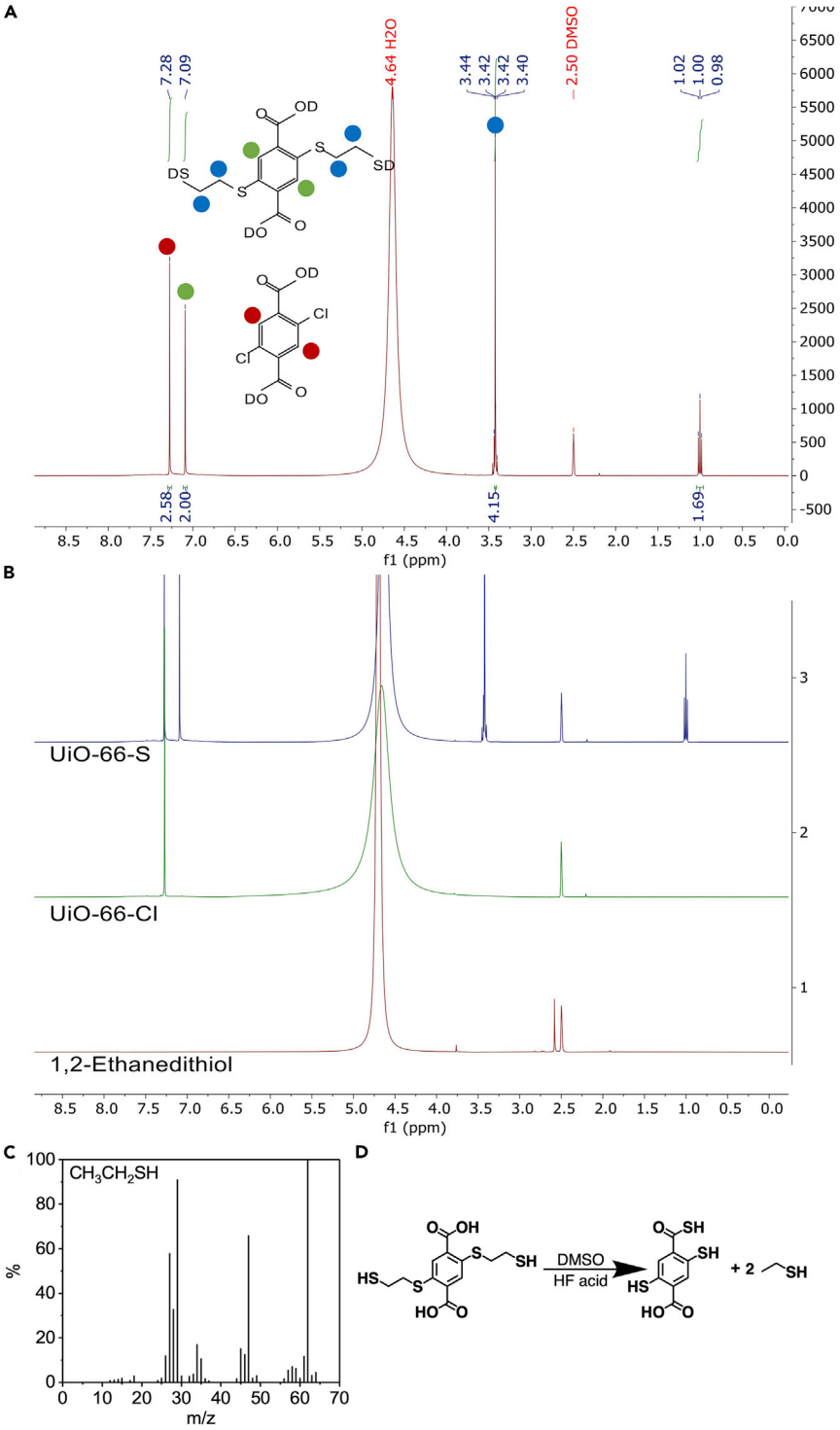

Figure 5. Digested NMR

(A) ^{1}H NMR spectra of the digested UiO-66-S.

(B) Stacked ^{1}H NMR spectra of the digested UiO-66-S, digested UiO-66-Cl, and 1,2-Ethanedithiol.

(C) Gas chromatography-mass spectrometry (GC-MS) of digested UiO-66-S.

(D) Proposed UiO-66-S digested in 0.4 mL DMSO and 0.2 mL NH_4F in H_2O stock solution (4.14 M). Reproduced with permission (Yuan et al., 2022); Copyright, 2022 Elsevier Inc.

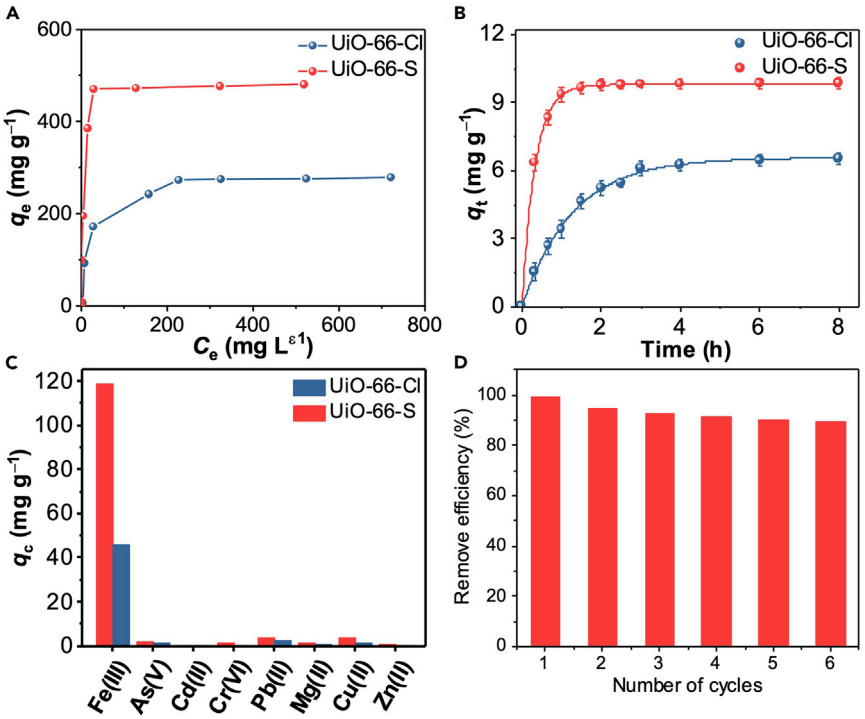

Figure 6. Adsorption performance of UiO-66 MOFs

(A) Uptake.

(B) Kinetics.

(C) Selectivity.

(D) Recyclability. Reproduced with permission (Yuan et al., 2022); Copyright, 2022 Elsevier Inc.

38. Before running the ICP-OES test, prepare three standard stock solutions, 5% HNO_3, 60 ppm, 125 ppm mix ion stock solution (Fe^{3+}, As (V) (AsO_4^{3-}), Cd^{2+}, Cr (VI) ($Cr_2O_7^{2-}$), Pb^{2+}, Mg^{2+}, Cu^{2+}, Zn^{2+}) for calibration.
39. If the R^2 values of all the calibration curves are larger than 0.9999, measure the Fe^{3+} concentration of the filtrate by ICP-OES (Figure 6C).

Ion adsorption – Recyclability tests

Timing: 198 h

After ion adsorption, we collect the MOFs powder to desorb the ion, which is used for another round of ion adsorption—repeating the adsorption/desorption cycles to analyze the recyclability of the MOFs.

40. Add 10 mg as-synthesized UiO-66-S to a 20 mL glass vial.
41. Mix 10 mL Fe^{3+} stock solution (10 ppm) with the MOFs.
42. Stir the mixture for 24 h.
43. Collect the filtrate by centrifuge, and measure the Fe^{3+} concentration by the ICP-MS.
44. Immerse the residual UiO-66-S in 10 mL citric acid (10 mM) for 9 h to desorption.
45. Wash the residual UiO-66-S with distilled water and anhydrous acetone and dry it in a vacuum oven overnight.
46. Use the regenerated UiO-66-S to measure the recyclability by repeating the adsorption/desorption process.

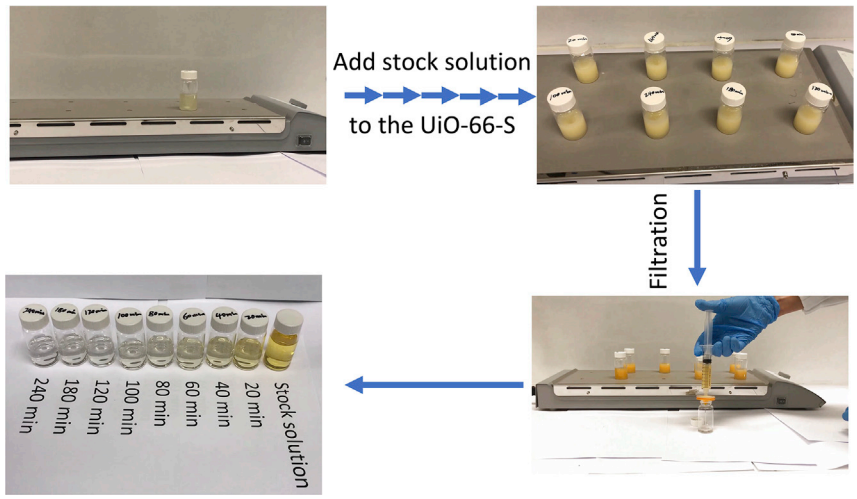

Figure 7. Procedure of Fe^{3+} adsorption kinetics measurement

500 ppm Fe^{3+} stock solution was used as such a high concentration of Fe^{3+} solution had a yellow color, and purification progress was visible to the eyes. Reproduced with permission (Yuan et al., 2022); Copyright, 2022 Elsevier Inc.

47. Before running the ICP-MS test, prepare the standard stock solution, 5% HNO_3, 2.5 ppm, 5 ppm, 7.5 ppm, and 10 ppm Fe^{3+} stock solution for calibration.
48. If the R^2 value of the calibration curve is larger than 0.9999, measure the Fe^{3+} concentration of the filtrate by ICP-MS (Figure 6D).

Adsorption process analysis

Timing: 24 h

49. Calculate the adsorption amount of Fe^{3+} using Equation 1,

$$q_e = \frac{(C_0 - C_e)\,V}{m} \quad \text{(Equation 1)}$$

where q_e (in mg g^{-1}) is the amount of Fe^{3+} adsorption at equilibrium, C_0 (in mg L^{-1}) is the initial concentration of the used stock solution, and C_e (in mg L^{-1}) is the measured concentration of the filtrate by the ICP-OES or ICP-MS. V (in L) is the volume of the solution used for measurement, and m (in mg) is the corresponding weight of the MOFs.

50. Use the Langmuir isotherm model and Freundlich isotherm model to analyze the adsorption process according to Equations 2 and 3. Treating the data collected from the uptake tests by the below two equations (Yao et al., 2022).

$$\frac{C_e}{q_e} = \frac{C_e}{q_{max}} + \frac{1}{q_{max} b} \quad \text{(Equation 2)}$$

$$\ln q_e = \ln K_f + \frac{1}{n} \ln C_e \quad \text{(Equation 3)}$$

where q_{max} is the maximum adsorption capacity. b and K_f are Langmuir constant and Freundlich constant, respectively. n is dimensionless exponent of Freundlich equation. Setting C_e as x-axis, C_e/q_e

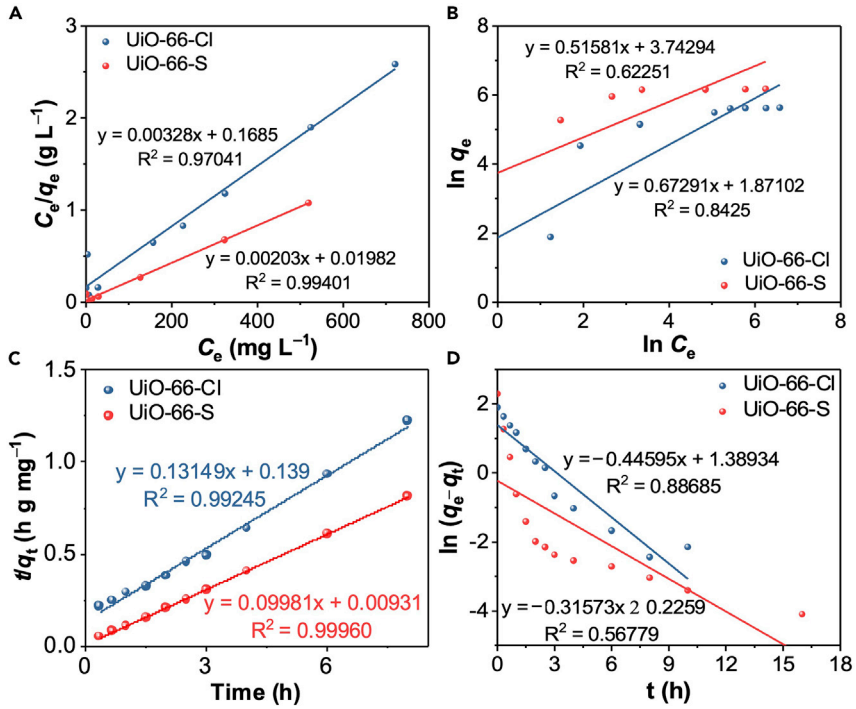

Figure 8. Adsorption performance and reaction model simulation of UiO-66 MOFs

(A) Langmuir model fitting according to Figure 6A.

(B) Freundlich model fitting according to Figure 6A.

(C) Pseudo-second-order model fitting according to Figure 6B.

(D) Pseudo-second-order model fitting according to Figure 6B. Reproduced with permission (Yuan et al., 2022); Copyright, 2022 Elsevier Inc.

as y-axis, using excel to linear fit the data collected from the uptake tests. According to Equation 2, the slope and intercept of the fitted curve correspond to the $1/q_{max}$ and $1/(q_{max}b)$, respectively. Then the maximum adsorption capacity was obtained.

51. Set $\ln(C_e)$ as an x-axis, $\ln(q_e)$ as a y-axis, using excel to linear fit the data collected from the uptake tests. According to Equation 3, the slope and intercept of the fitted curve correspond to the 1/n and $\ln(K_f)$, respectively.
52. Compare the R^2 values obtained from the fitted results of Equations 2 and 3. The Langmuir model describes the adsorption process of Fe^{3+} better (Figures 8A and 8B), indicating that the Fe^{3+} is adsorbed on the monolayer surface of MOFs and the adsorption process is uniform chemical adsorption.
53. Use the pseudo-first-order kinetic model and pseudo-second-order kinetic model to analyze the adsorption kinetics according to Equations 4 and 5, respectively.

$$\log(q_e - q_t) = \log(q_e) - \frac{k_1}{2.303}t \quad \text{(Equation 4)}$$

$$\frac{t}{q_t} = \frac{1}{k_2 q_e^2} + \frac{t}{q_e} \quad \text{(Equation 5)}$$

where q_t and q_e (in mg g^{-1}) are the amounts of Fe^{3+} adsorbed at time t and at equilibrium, respectively. k_1 (in min^{-1}) and k_2 (in g mg^{-1} h^{-1}) are the rate constant of pseudo-first-order and

pseudo-second-order adsorption, respectively. Setting t as x-axis, $\log(q_e\text{-}q_t)$ as y-axis, using excel to linear fit the data collected from the kinetics tests. According to Equation 4, the slope and intercept of the fitted curve correspond to the $-k_1/2.303$ and $\log(q_e)$, respectively. Then the rate constant k_1 was obtained.

54. Set t as an x-axis, t/q_t as a y-axis, using excel to linear fit the data collected from the kinetics tests. According to the Equation 5, the slope and intercept of the fitted curve correspond to the $1/q_e$ and $1/(k_2\ q_e^2)$, respectively. Then the rate constant k_2 was obtained.
55. Compare the R^2 values obtained from the fitted results of Equations 4 and 5. The Fe^{3+} adsorption matches well with the pseudo-second-order reaction model, which indicates the rate-limiting factor in the Fe^{3+} adsorption process depends on chemisorption. The rate constant k for UiO-66-S and UiO-66-Cl was calculated to be 1.07 and 0.124 g mg^{-1} h^{-1}, respectively (Figures 8C and 8D).

EXPECTED OUTCOMES

This protocol provides the procedure for MOFs synthesis and post-functionalization. The synthesized MOFs show high crystallinity and stability, which are stable in water (pH = 6.8) at room temperature for 35 days, demonstrating their feasibility for water purification application. The synthesized MOFs show Brunauer–Emmett–Teller (BET) surface area of 446 and 275 m^2 g^{-1} for UiO-66-Cl and UiO-66-S, respectively. Under practical operating temperatures, i.e., < 200°C, UiO-66-S shows improved thermal stability. In addition, the synthesized MOFs have been stable for more than a week under acidic conditions (0.1 mol L^{-1} HCl). Optimizing the reaction condition of post-functionalization, the maximum 52.13% of Cl was replaced by 1,2-Ethanedithiol after 48 h of reaction time, which shows the highest adsorption capacity.

UiO-66-S can remove Fe^{3+} with the highest adsorption capacity (481 mg g^{-1}) and fastest kinetics (1.07 g mg^{-1} h^{-1}) for water purification application. In addition, the UiO-66-S shows high selectivity toward Fe^{3+}. The removal efficiency of UiO-66-S remained at over 89% after six cycles demonstrating its high recyclability.

LIMITATIONS

Various conditions, including acidic, basic, and neutral, are common for the practical application of water purification. The synthesized MOFs in this protocol are stable in acidic and neutral conditions. However, it can only be stable in the basic condition (0.01 mol L^{-1} NaOH) for two days. Therefore, the synthesized MOFs are limited to extremely basic conditions. The reason is the coordination of the hydroxides with Zr^{4+}. This limitation can be improved by hydrophobic surface treatment, insertion of stabilizing pillars, and composite construction. See the reference for more detailed information (Ding et al., 2019).

TROUBLESHOOTING

Problem 1

The synthesized MOFs show low crystallinity (steps 1–4 in "MOFs synthesis").

Potential solution

Add modulators to the reaction solution, such as formic acid, acetic acid, and trifluoroacetic acid. The modulator could coordinate with the metal cluster and slow down the reaction leading to improved crystallinity.

Problem 2

The stock solution is used in the adsorption process (step 18 in "ion adsorption – uptake tests").

Potential solution

Iron can be easily precipitated by a hydrolytic mechanism. Therefore, the matrix used to prepare the stock solution must be acidic to ensure the existing iron is in an ion state. The potential solution for the stock solution preparation should be 5% HNO_3, which is clarified in the "before you begin" section.

Problem 3

The results obtained from ICP-MS were not good enough (step 31 in "ion adsorption – kinetic tests").

Potential solution

Prepare the stock solution more accurately. The 10 ppm stock solution should be diluted from the 1000 ppm stock solution. In addition, the R^2 values of the calibration curve should be larger than 0.9999, and then conduct the ICP-MS measurement.

Problem 4

Incomplete removal of unreacted starting material and DMF molecules (steps 6–8 in "activation of MOFs").

Potential solution

Replace the DMF and acetone in steps 6–8 more frequently. Alternatively, wash the MOFs by Soxhlet extraction with methanol and acetone as a solution, each solution for three days.

Problem 5

Low conversion efficiency of the post-functionalization (steps 9–17 in "post-functionalization of UiO-66-Cl to UiO-66-S").

Potential solution

Use anhydrous DMF as a solvent and set up the reaction under the inert gas atmosphere. The 1,2-Ethanedithiol (EDT) is air-sensitive and should be stored under inert gas.

RESOURCE AVAILABILITY

Lead contact

Further information and requests for resources and reagents should be directed to and will be fulfilled by the lead contact, Yoonseob Kim (yoonseobkim@ust.hk).

Materials availability

This study did not generate any new unique reagents.

Data and code availability

Data and code would be made available upon request.

SUPPLEMENTAL INFORMATION

Supplemental information can be found online at https://doi.org/10.1016/j.xpro.2022.101477.

ACKNOWLEDGMENTS

This work is supported by the Research Grants Council of the Hong Kong SAR Government (Early Career Scheme, 26309420), the Department of Chemical and Biomolecular Engineering, HKUST (startup funding), and the Guangdong Provincial International Cooperation Program (project number 2021A0505030018).

AUTHOR CONTRIBUTIONS

Y.K. conceived and supervised the project. Y.Y. designed and performed all the experiments and data analysis.

DECLARATION OF INTERESTS

The authors declare no competing interests.

REFERENCES

Area, M., Garau, A., Isaia, F., and Lippolis, V. (1996). Assignments of carbon-sulphur vibrations by selenation: an FT-IR and FT-Raman study on 1, 3, 5-trithiacyclohexane. Spectrosc. Lett. *29*, 697–709. https://doi.org/10.1080/00387019608007062.

Ding, M., Cai, X., and Jiang, H.-L. (2019). Improving MOF stability: approaches and applications. Chem. Sci. *10*, 10209–10230. https://doi.org/10.1039/C9SC03916C.

Duan, X., Wang, C., Wang, T., Xie, X., Zhou, X., and Ye, Y. (2018). A polysulfone-based anion exchange membrane for phosphoric acid concentration and purification by electro-electrodialysis. J. Membr. Sci. *552*, 86–94. https://doi.org/10.1016/j.memsci.2018.02.004.

Feng, M., Zhang, P., Zhou, H.-C., and Sharma, V.K. (2018). Water-stable metal-organic frameworks for aqueous removal of heavy metals and radionuclides: a review. Chemosphere *209*, 783–800. https://doi.org/10.1016/j.chemosphere.2018.06.114.

Gabarrón, S., Gernjak, W., Valero, F., Barceló, A., Petrovic, M., and Rodríguez-Roda, I. (2016). Evaluation of emerging contaminants in a drinking water treatment plant using electrodialysis reversal technology. J. Hazard Mater. *309*, 192–201. https://doi.org/10.1016/j.jhazmat.2016.02.015.

Hartmann, J., Braulke, F., Sinzig, U., Wulf, G., Maas, J.H., Konietschke, F., and Haase, D. (2013). Iron overload impairs proliferation of erythroid progenitors cells (BFU-E) from patients with myelodysplastic syndromes. Leuk. Res. *37*, 327–332. https://doi.org/10.1016/j.leukres.2012.11.005.

Huang, J.H., Cheng, X.Q., Zhang, Y., Wang, K., Liang, H., Wang, P., Ma, J., and Shao, L. (2020). Polyelectrolyte grafted MOFs enable conjugated membranes for molecular separations in dual solvent systems. Cell Rep. Phys. Sci. *1*, 100034. https://doi.org/10.1016/j.xcrp.2020.100034.

Hui, K., Chao, C., and Kot, S. (2005). Removal of mixed heavy metal ions in wastewater by zeolite 4A and residual products from recycled coal fly ash. J. Hazard Mater. *127*, 89–101. https://doi.org/10.1016/j.jhazmat.2005.06.027.

Khatri, N., Tyagi, S., and Rawtani, D. (2017). Recent strategies for the removal of iron from water: a review. J. Water Proc. Eng. *19*, 291–304. https://doi.org/10.1016/j.jwpe.2017.08.015.

Mohammadinezhad, A., and Akhlaghinia, B. (2019). CoII immobilized on an aminated magnetic metal–organic framework catalyzed C–N and C–S bond forming reactions: a journey for the mild and efficient synthesis of arylamines and arylsulfides. New J. Chem. *43*, 15525–15538. https://doi.org/10.1039/C9NJ03400E.

Nemati, M., Hosseini, S.M., and Shabanian, M. (2017). Novel electrodialysis cation exchange membrane prepared by 2-acrylamido-2-methylpropane sulfonic acid; heavy metal ions removal. J. Hazard Mater. *337*, 90–104. https://doi.org/10.1016/j.jhazmat.2017.04.074.

Sun, D.T., Peng, L., Reeder, W.S., Moosavi, S.M., Tiana, D., Britt, D.K., Oveisi, E., and Queen, W.L. (2018). Rapid, selective heavy metal removal from water by a metal–organic framework/polydopamine composite. ACS Cent. Sci. *4*, 349–356. https://doi.org/10.1021/acscentsci.7b00605.

Wang, J., Deng, B., Wang, X., and Zheng, J. (2009). Adsorption of aqueous Hg(II) by sulfur-impregnated activated carbon. Environ. Eng. Sci. *26*, 1693–1699. https://doi.org/10.1089/ees.2008.0418.

WHO (World Health Organization). (2003). Iron in Drinking-Water. Background Document for Preparation of WHO Guidelines for Drinking-Water Quality (World Health Organization). (WHO/SDE/WSH/03.04/8).

Yao, Z., Shao, P., Fang, D., Shao, J., Li, D., Liu, L., Huang, Y., Yu, Z., Yang, L., Yu, K., and Luo, X. (2022). Thiol-rich, porous carbon for the efficient capture of silver: understanding the relationship between the surface groups and transformation pathways of silver. Chem. Eng. J. *427*, 131470. https://doi.org/10.1016/j.cej.2021.131470.

Yuan, S., Feng, L., Wang, K., Pang, J., Bosch, M., Lollar, C., Sun, Y., Qin, J., Yang, X., Zhang, P., et al. (2018a). Stable metal–organic frameworks: design, synthesis, and applications. Adv. Mater. *30*, 1704303. https://doi.org/10.1002/adma.201704303.

Yuan, S., Qin, J.-S., Lollar, C.T., and Zhou, H.-C. (2018b). Stable metal–organic frameworks with group 4 metals: current status and trends. ACS Cent. Sci. *4*, 440–450. https://doi.org/10.1021/acscentsci.8b00073.

Yuan, Y., Yu, J., Chen, H., Bang, K.-T., Pan, D., and Kim, Y. (2022). Thiol-functionalized Zr metal-organic frameworks for efficient removal of Fe^{3+} from water. Cell Rep. Phys. Sci. *3*, 100783. https://doi.org/10.1016/j.xcrp.2022.100783.